Published online June 15, 2017

Meat and Muscle Biology™

Metabolite Profile Differences between Beef Longissimus and Psoas Muscles during Display

Anupam Abraham,[1] Jack W. Dillwith,[2] Gretchen G. Mafi,[1]
Deborah L. VanOverbeke,[1] Ranjith Ramanathan[1]*

[1]Department of Animal Science, Oklahoma State University, Stillwater, OK 74078, USA
[2]Department of Entomology and Plant Pathology, Oklahoma State University, Stillwater, OK 74078, USA
*Corresponding author. E-mail: ranjith.ramanathan@okstate.edu (R. Ramanathan)

Abstract: The objective of this research was to compare metabolite profiles between beef *longissimus* and *psoas* muscles during display. Beef short loins were collected 3 d postmortem ($n = 10$). Steaks were cut from each *longissimus lumborum* (LL) and *psoas major* (PM) muscle and displayed under retail conditions for 7 d. Surface color, biochemical properties, and metabolites were analyzed during storage. PM decreased in redness ($P < 0.05$) by d 3 of display compared with LL. There were differences in metabolite concentrations ($P < 0.05$) between each muscle type at each time point. Sugars, amino acids, tricarboxylic acid cycle intermediates, and glycolytic substrates were detected in both muscles. Glycolytic metabolites such as pyruvic acid, glucose–6–phosphate, and fructose were greater ($P < 0.05$) in LL than PM at all display times. On d 0, the intensity of pyruvic acid in LL and PM were 142 and 42, respectively. Citric acid and succinic acid were lower on d 0, but were greater ($P < 0.05$) in LL compared with PM by d 7 of display. Carnitine was lower ($P < 0.05$) in LL than PM at all display times. On d 7, carnitine level in LL was 4.1 while in PM was 13,500. The results suggest that in addition to muscle-specific differences in mitochondrial and enzyme activities, inherent metabolite differences also may contribute to muscle color stability.

Keywords: beef color, *longissimus lumborum*, mass spectrometry, metabolomics, *psoas major*
Meat and Muscle Biology 1:18–27 (2017) **doi:10.22175/mmb2016.12.0007**
Submitted 16 December 2016 Accepted 29 March 2017

Introduction

Myoglobin is a sarcoplasmic protein that is primarily responsible for meat color. In fresh meat, myoglobin can exist in 3 different redox forms, namely deoxymyoglobin, oxymyoglobin, and metmyoglobin (AMSA, 2012). Deoxymyoglobin imparts purple color while predominant oxymyoglobin gives consumers the preferred bright-red color to beef. Oxidation of both oxy- and deoxymyoglobin result in the formation of metmyoglobin and discoloration of meat (Faustman and Cassens, 1990). Although various pre- and post-harvest factors can increase myoglobin oxidation, meat has an inherent capacity to delay metmyoglobin accumulation by a process called metmyoglobin reducing activity (MRA; Ledward, 1985). The concentration of reduced nicotinamide adenine dinucleotide (NADH), myoglobin chemistry, and mitochondrial activity play a significant role in metmyoglobin reduction (Tang et al., 2005; Ramanathan and Mancini, 2010; Nerimetla et al., 2017). In postmortem muscle, enzymes involved in the glycolytic and tricarboxylic acid cycle (TCA) retain activity. However, the metabolite concentration decreases with postmortem time. Various studies have shown that the addition of metabolites such as lactate, pyruvate, and succinate to meat or isolated mitochondria can regenerate NADH and can influence beef color (Tang et al., 2005; Kim et al., 2006; Ramanathan et al., 2011). Therefore, characterizing TCA and glycolytic substrate changes in postmortem muscle is critical to understand the fundamental basis for meat discoloration.

This research was supported by the Agriculture and Food Research Institute Grant 2014–67018–21646 from the USDA National Institute of Food and Agriculture program [Accession Number: 1001214].

Muscles in a beef carcass can be classified as color-stable or color-labile depending on the proportion of red and white fibers. *Longissimus lumborum* (LL), which is commonly merchandised as New York strip steak, is a color-stable muscle while the tenderloin (*Psoas major*; PM*)* is a color-labile muscle (O'Keeffe and Hood, 1982; Seyfert et al., 2007). Various researchers have shown that biochemical properties such as MRA and oxygen consumption rate can vary between LL and PM (McKenna et al., 2005). A recent study suggests that the sarcoplasmic proteome differs significantly between LL and PM (Joseph et al., 2012). More specifically, an overabundance of enzymes involved with color stability such as aldose reductase, pyruvate dehydrogenase, β-enolase, and triose phosphate isomerase involved in the glycolytic pathway were reported in LL compared to PM. Muscles with more red muscle fibers (PM) will have more mitochondria and capillary density than muscles with more white fibers (LL). Hence TCA and glycolytic substrates will be utilized at different rates in red muscles than in white muscles (Kushmerick et al., 1992; Glancy and Balaban, 2011). Recently metabolomics was used to study color stability in ovine meat (Subbaraj et al., 2016). However, limited studies have utilized metabolomic techniques to characterize beef color. Therefore, the objective of this study was to determine the metabolomic profile differences between LL and PM using a gas chromatography-mass spectrometry-based metabolomics approach to gain insights into muscle-specific differences in color stability.

Materials and Methods

This research did not include animal or human subjects and therefore does not require Animal Care and Use Committee approval.

Raw materials and processing

Ten USDA Choice short loins were purchased from a major packing facility 3-d postmortem. Vacuum packaged loins were transported on ice to the Robert M. Kerr Food and Agricultural Products Center at Oklahoma State University. Ten beef strip loins (*longissimus lumborum;* IMPS #180) and 10 tenderloins (*psoas major*; IMPS #190A) were separated from each short loin, and each was cut into five 2.5-cm-thick steaks using a meat slicer (Bizerba USA Inc., Piscataway, NJ). The steaks were placed onto foam trays with absorbent pads, overwrapped with PVC film (oxygen-permeable polyvinyl chloride fresh meat film; 15,500–16,275 cm^3 O_2/m^2 per 24 h at 23°C, E-Z Wrap Crystal Clear Polyvinyl Chloride Wrapping Film, Koch Supplies, Kansas City, MO) and stored in a simulated retail display under fluorescent lighting for 7 d. The surface color was measured daily using a HunterLab Miniscan spectrophotometer (HunterLab Associates, Reston, VA). Following surface color measurements, steaks were cut in half. The first half was used to measure metmyoglobin reducing activity (MRA) and oxygen consumption (OC), and the second half was used to measure metabolite profile and pH. The steak half assigned to MRA and OC was then bisected parallel to the oxygenated surface to expose the interior of steak (resulting in 2 interior pieces). The first interior section was used to measure MRA and the second interior piece was used to measure OC. From the second half, representative samples that contained both oxygenated and interior sections were taken for both metabolomics and pH measurements.

Muscle pH

Ten grams of LL and PM steak samples were blended with 100 mL of deionized water at 25°C, and homogenized for 30 s in a Sorvall Omni tabletop mixer (Newton, CT). The pH of the muscle homogenates was measured using an Accumet combination glass electrode connected to an Accumet 50 pH meter (Fisher Scientific, Fairlawn, NJ).

Retail display

After packaging, steaks were placed in a coffin-style open display case maintained at 2°C ± 1 under continuous lighting (1,612 to 2,152 lux, Philips Deluxe Warm White Fluorescent lamps; Andover, MA; color rendering index = 86; color temperature = 3,000° K). All packages were rotated daily to minimize the effects of variation in light intensity or temperature due to location.

Surface color measurement

At each display time, the surface color was measured on the steaks assigned to that display time at 2 random locations using a HunterLab MiniScan XE Plus spectrophotometer (HunterLab Associates) with a 2.5-cm diameter aperture, illuminant A, and 10° standard observer. Reflectance (R) at isobestic wavelengths from 400 to 700 nm was used to quantify myoglobin redox forms on the surface of steaks. Reflectance at 474, 525, 572, and 610 nm was converted to K/S values using the following equation: $K/S = (1-R)^2/2R$. These values were then substituted into the appropriate equations (AMSA, 2012) to calculate the percentage of deoxymyoglobin (DeoxyMb), oxymyoglobin (OxyMb), or

metmyoglobin (MetMb). Percentage myoglobin form values also were used to calculate MRA and OC.

Metmyoglobin Reducing Activity (MRA)

Metmyoglobin reducing activity was determined according to the procedure described by Sammel et al. (2002). Samples from the interior of steak halves were submerged in a 0.3% solution of sodium nitrite for 20 min (Sigma Aldrich Corp., St. Louis, MO) to facilitate MetMb formation, and then removed, blotted dry, vacuum packaged (Prime Source Vacuum Pouches, 4 mil, Koch Supplies Inc., Kansas City, MO), and scanned with a HunterLab MiniScan XE Plus spectrophotometer to determine pre-incubation MetMb values (AMSA, 2012). Each sample was incubated at 30°C for 2 h to induce MetMb reduction. Upon removal from the incubator, samples were rescanned to determine the percentage of remaining surface MetMb. The following equation was used to calculate MRA: (% surface MetMb pre-incubation – % surface MetMb post-incubation). Increased MRA is associated with improved color stability.

Oxygen consumption (OC)

Oxygen consumption was determined according to a modified procedure of Madhavi and Carpenter (1993), on the fresh-cut surface of the bottom half portion of the cube removed prior to MRA analysis. The samples were allowed to oxygenate for 30 min at 1°C, vacuum packaged, and then scanned twice (as described in the MRA procedure) on the bloomed surface (representing the previously unexposed interior of the original cube) to measure OxyMb. The surface color was measured through the vacuum packaging. The instrument was also standardized using the same packing material. Oxygen consumption (measured by conversion of OxyMb to DeoxyMb) was induced by incubating samples at 30°C for 30 min. Samples were rescanned immediately on removal to determine remaining surface OxyMb as a percentage by using K/S ratios and equations (AMSA, 2012). To calculate OC, changes in OxyMb values pre- and post-incubation were used.

Metabolomic analysis

Sample preparation. The metabolites were extracted from the muscle samples, following a modified procedure of Brown et al. (2012). Briefly, 0.5 g of intact muscle was kept in 1.5 mL of methanol (GC–MS grade, J.T Baker, Pittsburgh, PA) in borosilicate glass vials with PTFE-lined caps. The vials were then vortexed for 30 s and incubated for 20 h at room temperature (22 to 26°C). Following incubation, the samples were vortexed for 10 s and centrifuged for 5 min at 2,000 rpm. From the supernatant, 200 µL was transferred to amber colored vials, and 2 µg ribitol was added as an internal standard. The samples were then dried under a gentle stream of nitrogen gas.

Metabolomic profiling. The metabolomic profiling was done using a gas chromatograph–mass spectrometer [GC–MS; Agilent 6890 GC coupled with a 5973N mass selective detector (MSD); Agilent Technologies, Palo Alto, CA]. Samples were derivatized before GC–MS analysis using a modified procedure described by Rudell et al. (2008). The dried samples were reconstituted with 100 µL methoxyamine (2% methoxyamine hydrochloride in pyridine; Rockford, PA) and incubated at 50°C for 2 h. Silylation was performed with 100 µL of *N*, *O*-bis (Trimethylsilyl) trifluoroacetamide with 1% trichloromethylsilane (BSTFA + 1% TMCS; Thermo Scientific, Waltham, MA) and incubated for 30 min at 50°C. After incubation, the mixture was transferred to glass vials containing deactivated polyspring glass inserts before analysis.

One microliter of the extract was injected using an Agilent 7683B auto sampler injector in splitless mode into an Agilent 6890 GC coupled with a 5973N MSD (Agilent Technologies). The temperature of the inlet was set at 250°C to vaporize the sample, and a splitless glass liner with a tapered bottom was used to focus the vapors to a DB-5MS GC capillary column (Agilent Technologies; 30 m × 250 µm × 0.25 µm). Ultra-pure helium (Stillwater Steel Supplies, Stillwater, OK) was used as a carrier gas at constant flow mode (1 mL/min). The oven was set to an initial temperature of 50°C for 5 min followed by a ramp of 5°C/min to a final temperature of 315°C, which was held for 3 min. The MSD was operated in electron ionization mode with transfer line and source temperatures maintained at 230°C and quadrupole temperature maintained at 106°C. Mass spectra ranging from m/z 50 to 650 were recorded in scan mode. Data were then processed by the MSD Chemstation (Agilent Technologies).

Statistical analysis

The experimental design was a split-plot with randomized block design in the whole plot (n = 10 replications). Each short loin from an animal served as a block. Within the whole plot, 10 LL and 10 PM muscles were considered as experimental units. Within the subplot, each LL and PM muscle was divided into five 1-inch steaks and randomly assigned to 0, 1, 3, 5, and 7 d (split-plot experimental unit). The fixed effects for the whole

plot included muscle type (LL or PM) and random effects included error A (muscle × unit). The fixed effects for the sub-plot included display time, muscle type × display time interaction, and random effects were residual error (Error B). Surface color, pH, MRA, and OC were analyzed as a split-plot design. Type-3 tests of fixed effects for muscle, display time, and their interactions were performed using the MIXED PROC of SAS (Version 9.3. SAS Inst. Inc., Cary, NC). Least square means for the protected F-tests ($P < 0.05$) were separated using the PDIFF option and were considered significant at $P < 0.05$.

Metabolomics data from the Chemstation were deconvoluted using an Automated Mass Spectral Deconvolution and Identification System (AMDIS) program. To extract good quality data, the signal to noise ratio was set at 20, with medium settings for resolution, sensitivity, and shape requirements. A new mass spectral library was created by combining mass spectral data of compounds included in the Fiehn Metabolomics RTL Library (Agilent Technologies) and the NIST 05 library (National Institute of Standards and Technology, Gaithersburg, MD). The compounds in the samples were identified by matching the mass spectra with those in the newly created library with the minimum match factor set at 80, to rule out any possible false positives. Peak alignment, normalization, and statistical analysis of the identified compounds were performed using an Agilent Mass Profiler Professional (MPP) software (Agilent Technologies).

The intensity of the detected masses was normalized using the internal standard (ribitol), and log transformed followed by baseline transformation to the median of all samples. The compounds identified in only one sample were then omitted, and to further increase the quality of the data, only those which were present in at least 50% of samples in one condition were selected for statistical analysis. The compounds identified by AMDIS using the mass spectra of the libraries (Fiehn Metabolomics RTL Library and NIST 05) were analyzed to determine significantly different compounds based on the normalized intensity values in the samples using the MPP. Two-way ANOVA ($P < 0.05$) was used to find the statistical significance of differences, and to further increase the data quality, Benjamini-Hochberg multiple test corrections ($P < 0.05$) were applied. An unsupervised principal component analysis (PCA) and hierarchical clustering analysis (HCA) were performed to differentiate the muscle type depending on metabolites. The normalized metabolites were clustered based on muscle type and intensities using Euclidean distance and Ward's linkage rule. Our initial analysis indicated that there were no significant differences in metabolite levels between d 0 and 1. Similarly, between d 3 and 5. To avoid the complexity of data analysis and the result presentation, metabolite levels in d 0, 3, and 7 were considered.

Results and Discussion

The enzymes involved in glycolysis and TCA cycle remain active in postmortem muscles. However, substrates required to regenerate reducing equivalents are depleted continuously. Hence, characterizing the metabolite changes using the traditional wet-laboratory methods can be challenging. We utilized a GC–MS based non-targeted metabolomics approach to study metabolome profile changes in LL and PM muscles. Metabolomic techniques allow simultaneous detection of hundreds of low molecular weight metabolites such as sugars, amino acids, nucleosides, fatty acids and other compounds such as nucleotides in a biological system (Kanani et al., 2008). The application of metabolomics has been applied in diverse research areas such as human medicine, drug discovery, plant science, human nutrition, and food science (Kaddurah-Daouk and Krishnan, 2008; Wishart, 2008; Cevallos-Cevallos et al., 2009). Few studies have utilized metabolomics techniques to characterize the role of metabolites in meat tenderness and water-holding capacity (Bertram et al., 2010; Graham et al., 2010; D´Alessandro et al., 2011; Warner et al., 2015).

There was a significant muscle type main effect for pH. *Psoas major* had greater ($P < 0.05$) pH than LL (PM = 5.72, LL = 5.61, SE = 0.02). As expected, PM discolored quickly compared with LL. By d 3 of display, PM had

Table 1. Redness (a* values), metmyoglobin reducing activity (MRA), and oxygen consumption (OC) for *longissimus lumborum* (LL) and *psoas major* (PM) during simulated retail display

Trait	Muscle type	Days of display 0	1	3	5	7	SE[1]
Redness	LL	$30.6^{a,x}$	$33.4^{b,x}$	$30.1^{a,x}$	$28.4^{c,x}$	$26.4^{d,x}$	0.2
	PM	$29.5^{a,y}$	$32.4^{b,y}$	$20.3^{c,y}$	$15.4^{d,y}$	$13.1^{e,y}$	
MRA	LL	$65.4^{a,x}$	$63.2^{a,x}$	$62.4^{ab,x}$	$58.4^{bc,x}$	$54.1^{c,x}$	2.4
	PM	$71.0^{a,y}$	$60.4^{b,x}$	$55.2^{c,y}$	$50.2^{d,y}$	$49.3^{d,y}$	
OC	LL	$60.2^{a,x}$	$55.8^{b,x}$	$48.6^{c,x}$	$44.2^{cd,x}$	$40.3^{d,x}$	2.8
	PM	$65.8^{a,y}$	$54.2^{b,x}$	$40.5^{c,y}$	$36.7^{d,y}$	$30.1^{e,y}$	

[a–e]Least squares means within a row with a different superscript letter differ ($P < 0.05$).

[x,y]Least squares means within a column and trait with a different superscript letter differ ($P < 0.05$).

[1]SE = standard error for muscle type × display time interaction.

lower redness compared with LL (Table 1). The changes in redness during display were greater ($P < 0.05$) for PM (d 7 – d 0 = 16.4 a* units) than LL (d 7 – d 0 = 6.2 a* units). Interestingly, both OC and MRA were greater ($P < 0.05$) for PM on d 0 of display than LL (Table 1). However, OC and MRA decreased more rapidly for PM by d 3 of display than LL. This suggests that oxidative changes were greater for PM than LL. Previous studies have reported color-labile nature of PM when compared with LL (McKenna et al., 2005; Joseph et al., 2012).

The concentration of muscle fiber types can influence the capillary network and metabolite use for cellular metabolism. Further, metabolism of carbohydrates, amino acids, and fatty acids are inter-related. Nevertheless, metabolism of carbohydrates can be attributed to the generation of reducing equivalents such as NADH and FADH (flavin adenine dinucleotide reduced). Mitochondrial content is greater in PM than LL (Mohan et al., 2010; Ramanathan et al., 2015) which can significantly influence the utilization of metabolites postmortem. One hundred and forty-one metabolites were identified in LL and PM. In the current study, an intensity difference of 2-log fold was considered significant, and 29 compounds were different ($P < 0.05$) after Benjamini-Hochberg multiple test correction. Of these, 19 compounds were found to have a fold change difference greater than 2 on a logarithmic scale. The significantly different metabolites between muscles across all display times are presented in Table 2, with P-value (after Benjamini-Hochberg correction), mass and retention time.

The principal component analysis scores plot (Fig. 1) clearly displayed the separation of metabolites between

Table 2. Metabolites differentially abundant in *longissimus lumborum* (LL) and *psoas major* (PM) during d 0, 3, and 7 of display

Metabolites	P-value	Mass	Retention time	CAS[1] number
Nucleoside metabolites				
Uracil	4.92×10^{-12}	241	28.277632	66–22–8
Hypoxanthine	0.0473757	265	39.709084	68–94–0
Carbohydrate metabolites and intermediates				
Fructose	1.04×10^{-12}	73	40.72578	57–48–7
Gluconic acid	1.32×10^{-12}	73	43.307842	526–95–4
D-malic acid	4.14×10^{-12}	73	32.104206	617–48–1
Citric acid	1.77×10^{-12}	273	39.673515	5949–29–1
D-glucose-6-phosphate	0.0010929	387	49.11201	56–73–5
Ribonic acid-gamma-lactone	0.0015542	73	36.767242	8–3-5336
1,3-dihydroxyacetone	0.003798	73	25.780489	96–26–4
Succinic acid	0.009169	147	27.61917	29915–38–6
D-ribose-5-phosphate	0.01282	315	45.262295	15673–79–7
Pyruvic acid	0.0389019	73	19.87522	127–17–3
Maltose	0.042729	361	55.512077	69–79–4
Amino acid metabolites and intermediates				
L-methionine	4.68×10^{-12}	176	33.021603	63–68–3
Hypotaurine	0.0027508	188	35.004578	300–84–5
Aspartic acid	0.003775	232	32.967148	56–84–8
L-carnitine	0.0139388	195	37.45107	541–15–1
L-valine	0.0285909	72	21.183283	72–18–4
Fatty acid metabolites and intermediates				
Glyceric acid	4.00×10^{-12}	73	27.939327	473–81–4
Palmitoleic acid	8.50×10^{-12}	311	44.014893	373–49–9
Linoleic acid	0.0019479	337	47.43296	60–33–3
Stearic acid	0.0023763	341	47.95428	57–11–4
Palmitic acid	0.0220514	313	44.391453	64519–82–0

[1]CAS = Chemical Abstracts Service.

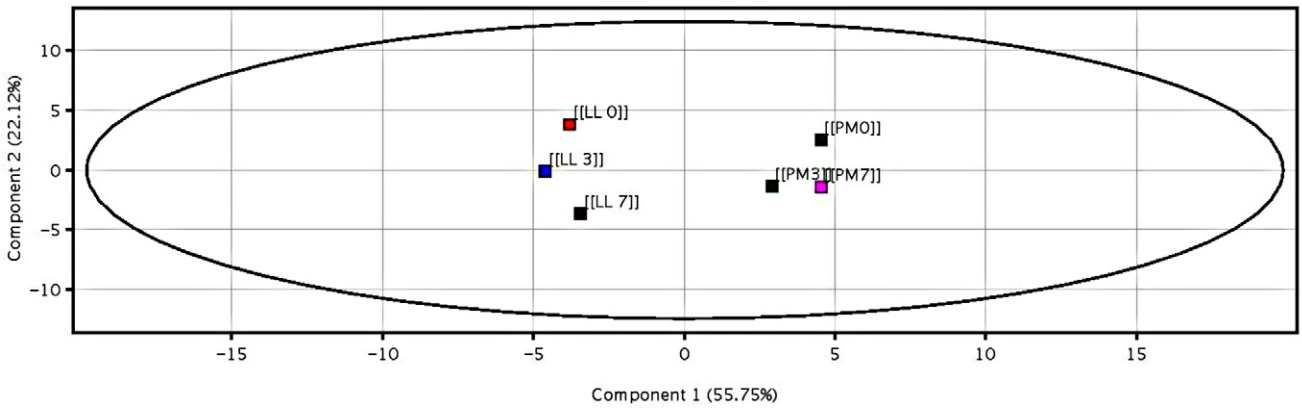

Figure 1. The PCA score plots of differentially abundant metabolites[1] in longissimus and psoas muscle during display time with Hotelling's T2 ellipse (95% confidence interval). [1]Total quantitative variances of 29 annotated peaks were clustered to reveal the difference and relative similarities of metabolite profiles of muscle type during display time. X-axis represents principal component 1 and Y-axis represents principal component 2.

LL and PM muscles. Both LL and PM were clustered separately. Positive loadings on the PC1 axis were obtained for PM while negative loadings were obtained for LL. The component 1 explains 55.75% variation in metabolite changes between samples (across muscles and display times) while the component 2 explains 22.12% of the variation. Further, the PCA plot indicates LL metabolite separation among d 0, 3, and 7 for the component 2. However, for PM, d 3 and 7 had little separation compared to d 0 across component 2. From the loadings plot the metabolites responsible for maximum variation were identified and the absolute loading values for component 1 are provided in Table 3. Uracil, hypoxanthine, malic acid, carnitine, and dihydroxy acetone had positive loadings indicating their effect on PM; whereas fructose, glucose–6–phosphate, methionine, and succinic acid had negative loadings explaining their influence on LL.

To visualize the metabolite changes during display, heat maps (Fig. 2) were plotted for metabolites that were different ($P < 0.05$). The heat map helps to view the changes in intensity levels of metabolites over the display time and between samples. The hierarchical clustering analysis indicated that there were differences between LL and PM as they sorted into different clusters (Fig. 3 and 4). The clustering analysis classifies the samples based on their similarities in metabolite intensity levels. In the

Table 3. Metabolites with their weighted loadings and absolute loadings for the principle component 1 (PC1)

Metabolites[1]	Component 1 (55.75%)	Absolute value
Uracil	0.24776196	0.24776196
Hypotaurine	0.24589851	0.24589851
L-carnitine	0.24571924	0.24571924
D-malic acid	0.23598695	0.23598695
Palmitoleic acid	0.23324004	0.23324004
Hypoxanthine	0.23120116	0.23120116
Fructose	–0.22991428	0.22991428
D-glucose-6-phosphate	–0.22124898	0.22124898
1,3-dihydroxyacetone	0.2190422	0.2190422
Stearic acid	0.21383685	0.21383685
Aspartic acid	0.20664789	0.20664789
D-ribose-5-phosphate	0.20287064	0.20287064
L-methionine	–0.18120633	0.18120633
L-valine	–0.16892305	0.16892305
Linoleic acid	0.1612704	0.1612704
Glyceric acid	–0.16115013	0.16115013
Palmitic acid	0.14535612	0.14535612
Succinic acid	–0.14027472	0.14027472
Citric acid	0.05239423	0.05239423
Pyruvic acid	–0.042259008	0.042259008
Ribonic acid-gamma-lactone	0.023172794	0.023172794
Maltose	–0.007306586	0.007306586

[1]Metabolites (P value < 0.05) with a fold change of 2 on a logarithmic scale are presented.

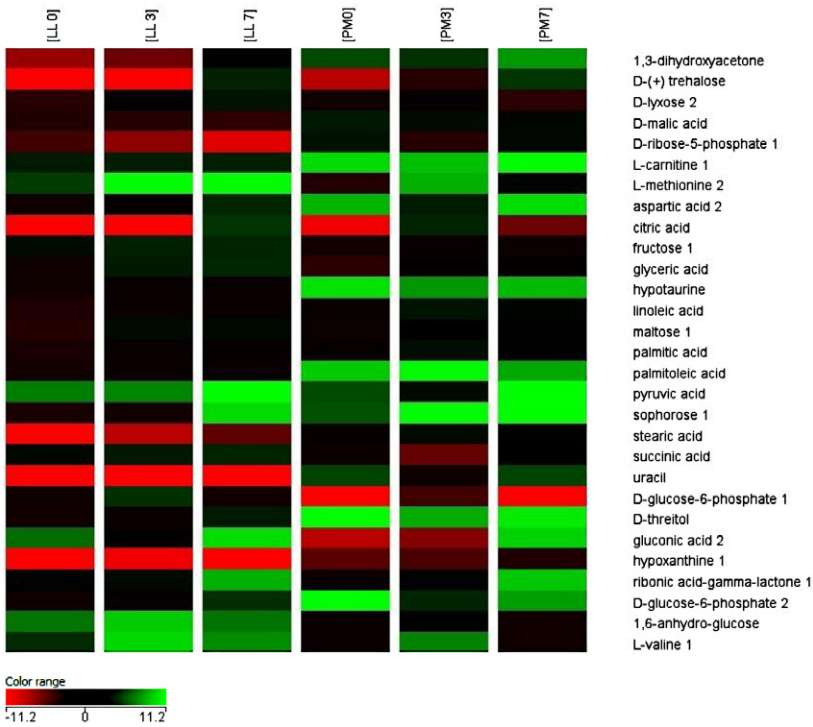

Figure 2. Heat map showing the changing patterns in metabolite concentrations based on normalized intensity values across muscle type and display time. The metabolites were normalized against the abundance of internal standard ribitol. The red color indicates lesser abundance and green color indicates a higher abundance. LL0 = *longissimus lumborum* on d 0, LL3 = *longissimus lumborum* on d 3, LL7 = *longissimus lumborum* on d 7, PM0 = *psoas major* on d 0, PM3 = *psoas major* on d 3, PM7 = *psoas major* on d 7.

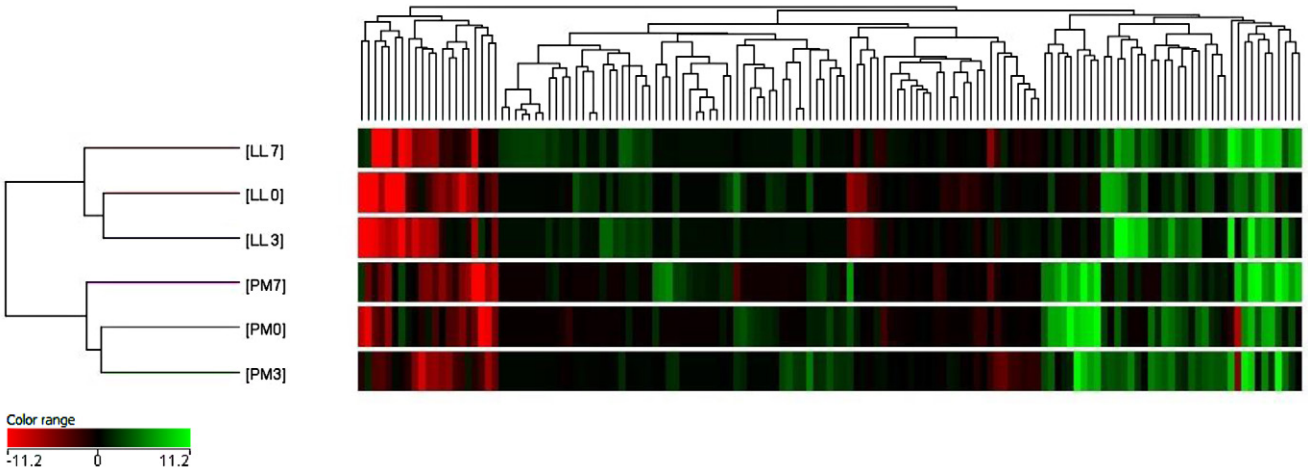

Figure 3. Hierarchical clustering of all identified metabolites from longissimus and psoas muscles during display time. Rows indicate muscle type and day of display, and columns indicate metabolites. Clustered based on metabolites normalized against the abundance of internal standard ribitol. The red color indicates lesser abundance and green color indicates a higher abundance. LL0 = *longissimus lumborum* on d 0, LL3 = *longissimus lumborum* on d 3, LL7 = *longissimus lumborum* on d 7, PM0 = *psoas major* on d 0, PM3 = *psoas major* on d 3, PM7 = *psoas major* on d 7.

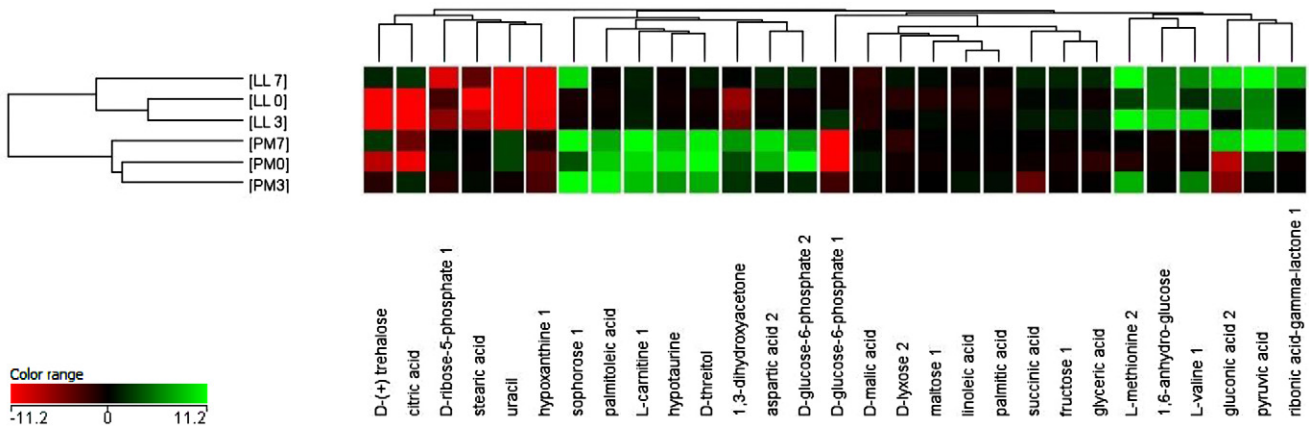

Figure 4. Hierarchical clustering of significantly different metabolites from longissimus and psoas muscles during display time. Rows indicate muscle type and day of display, and columns indicate metabolites. The metabolites were normalized against the abundance of internal standard ribitol. The red color indicates lesser abundance and green color indicates a higher abundance. LL0 = *longissimus lumborum* on d 0, LL3 = *longissimus lumborum* on d 3, LL7 = *longissimus lumborum* on d 7, PM0 = *psoas major* on d 0, PM3 = *psoas major* on d 3, PM7 = *psoas major* on d 7.

current study, LL and PM were grouped into 2 different clusters indicating a difference in metabolite intensity levels. For both LL and PM, metabolite clusters were similar on d 0 and 3, but were different on d 7.

Glycolytic compounds (fructose, glucose–6–phosphate, pyruvic acid) were abundant in LL (Tables 4 and 5) than PM. Previous research also indicated that color stable muscles have predominantly glycolytic metabolism (O'Keeffe and Hood, 1982; Joseph et al., 2012). Citric acid was greater in PM on d 0 and 3 compared with LL. However, on d 7, citrate levels were greater in LL than PM. This can be attributed to the utilization of citrate in PM for mitochondrial activity. A previous study indicated that pyruvate dehydrogenase was overabundant in color stable muscle (Joseph et al., 2012). This suggests that in LL, pyruvate may be entering the Krebs cycle, and thereby, increasing citrate levels. Further, PM has a higher mitochondrial aconitase (an enzyme that converts citrate to isocitrate; Joseph et al., 2012), which may be another reason for the lower level of citrate in PM.

Succinate is a complex II substrate and is an intermediate metabolite in the TCA cycle. The addition of succinate can limit MetMb formation by electron transport mediated metmyoglobin reduction (Tang et al., 2005) and also by reverse electron transport (Belskie et

Table 4. Differential abundance[1] of metabolites[2] in *longissimus lumborum* (LL) compared to *psoas major* (PM) on d 0, 3, and 7 of display

Compound	d 0	d 3	d 7
1,3-dihydroxyacetone	down	down	down
D-malic acid	down	down	down
D-ribose-5-phosphate	down	down	down
L-carnitine	down	down	down
Aspartic acid	down	down	down
Citric acid	down	down	**
Hypotaurine	down	down	down
Linoleic acid	down	down	**
Palmitoleic acid	down	down	down
Stearic acid	down	down	down
Uracil	down	down	down
Hypoxanthine	down	down	down
D-threitol	down	**	**
Ribonic acid-gamma-lactone	**	**	down
L-methionine	up	up	up
Fructose	up	up	up
Citric acid	**	**	up
Glyceric acid	up	up	up
Pyruvic acid	up	up	**
D-glucose-6-phosphate	up	up	up
L-valine	up	**	up
Succinic acid	**	up	up

**Represents no changes ($P > 0.05$) were detected.

[1]Metabolites ($P < 0.05$) with a fold change of 2 on a logarithmic scale are presented.

[2]Down represents on a specific day (either 0, 3, or 7) metabolite level in LL was lower compared with PM. Similarly, up represents on a specific day (either 0, 3, or 7) metabolite level in LL is greater compared with PM.

al., 2015). On d 3 and 7, succinate levels in PM were lower than LL (Tables 4 and 5). Hence, rapid discoloration in PM can be attributed to lower levels of succinate. Greater levels of succinate in LL can be due to (1) less utilization by mitochondria and (2) formation from glutamic acid or valine. In the current study, valine content in LL was greater than PM. However, further research is necessary to validate the conversion of valine to succinate in postmortem muscles.

The amino acid derivative carnitine is involved in transporting fatty acids into mitochondria for oxidation. *Psoas major* had greater carnitine levels compared to LL. This can be due to greater mitochondrial content in PM than LL. In contrast to the findings of Subbaraj et al. (2016), methionine levels were higher in LL. Hypotaurine, a metabolic breakdown product of cysteine and methionine metabolism, was lower in LL. Therefore, it is possible that PM and LL differ in cysteine-methionine metabolism. Joseph et al. (2012) reported that greater levels of methionine sulfoxide reductase prevented oxidation of methionine in longissimus than psoas muscles. In the current study, a greater concentration of methionine sulfoxide reductase may have increased methionine level in LL than PM.

Nucleotide degradation rate varied between muscle type. For example, there were differences in hypoxanthine and ribose–5–phosphate levels between LL and PM. These compounds are formed from the hydrolysis of inosine–5–monophosphate by nucleosidases (Koutsidis et al., 2008). Hypoxanthine can

Table 5. List of metabolites with their intensity values and *p* values after Benjamini-Hochberg correction

	Intensity values[1]						
Metabolites	LL0	PM0	LL3	PM3	LL7	PM7	*P*-value[2]
Nucleoside metabolites							
Hypoxanthine	142	9.49×10^5	4.02×10^3	1.06×10^6	1.77×10^3	7.57×10^6	0.09
Inosine	2.14×10^7	4.03×10^7	5.66×10^7	6.28×10^6	8.51×10^5	3.32×10^6	0.31
Uracil	2.63	9.06×10^5	3.24	4.43×10^4	10.6	1.08×10^6	< 0.0001
Xanthine	179	1.91×10^3	9.41×10^3	2.24×10^3	1.04×10^3	1.45×10^4	0.68
Myo-inositol	2.66×10^7	4.90×10^7	2.78×10^7	3.22×10^7	3.02×10^7	4.78×10^7	0.89
Inosine 5'-monophosphate	3.82	1*	16.3	1*	1*	1*	0.20
Amino acid metabolites							
Hypotaurine	1*	3.42×10^3	1*	2.13×10^2	1*	1.24×10^3	0.01
Aspartic acid	1*	7.78×10^2	1*	3.67	4.48	3.59×10^3	0.01
L-alanine	1.71×10^7	3.37×10^7	2.36×10^7	3.66×10^6	2.27×10^7	4.03×10^7	0.58
L-carnitine	3.81	2.85×10^3	3.56	7.96×10^2	4.19	1.35×10^4	0.03
L-cysteine	3.55	3.93	1.46×10^2	474	17.3	3.07×10^3	0.30
L-glutamic acid	1.20×10^4	1.98×10^6	3.06×10^5	2.70×10^4	1.01×10^6	2.55×10^4	0.34
L-methionine	12.7	1*	8.00×10^5	5.45×10^2	9.18×10^5	4.03	< 0.0001
L-ornithine 2	3.82	4.07	1*	1*	1*	1*	0.79
L-proline	1.91×10^6	2.16×10^6	2.47×10^6	3.83×10^5	2.16×10^6	2.09×10^6	0.75

Continued

Continued

Metabolites	Intensity values[1]						*P*-value[2]
	LL0	PM0	LL3	PM3	LL7	PM7	
L-valine	3.5	1*	729	60.1	19	1*	0.04
Carbohydrate metabolites							
Citric acid	56	1.82×10^2	21.1	8.62×10^5	9.95×10^5	1.68×10^4	3.28×10^{-4}
Creatinine	2.63×10^7	1.28×10^8	4.31×10^6	8.32×10^7	1.83×10^8	1.52×10^8	0.70
D-glucose	6.73×10^7	5.32×10^7	7.85×10^7	6.65×10^7	8.27×10^7	2.06×10^7	0.29
D-erythrose-4-phosphate	9.98×10^3	3.29×10^3	7.93×10^2	8.32×10^2	2.98×10^2	31.4	0.37
D-glucose-6-phosphate	1.21×10^7	1.02×10^3	6.67×10^7	2.38×10^6	7.73×10^6	2.73×10^3	0.002
D-malic acid	1.91×10^6	1.73×10^7	1.32×10^6	7.36×10^6	8.94×10^5	1.11×10^7	< 0.0001
D-ribose-5-phosphate	1.08×10^5	2.22×10^6	7.64×10^3	2.54×10^5	9.99×10^2	1.96×10^6	0.02
Fructose	6.01×10^7	3.50×10^7	9.95×10^7	3.33×10^7	1.12×10^8	5.40×10^7	< 0.0001
Fumaric acid	2.26×10^4	3.36×10^6	1.49×10^4	9.19×10^5	7.10×10^4	1.96×10^6	0.13
L-(+) lactic acid	1.08×10^5	3.86×10^6	2.13×10^8	2.84×10^7	3.23×10^7	4.74×10^6	0.40
Malonic acid	2.15×10^5	7.05×10^4	4.93×10^2	1.32×10^2	3.32×10^3	6.93×10^3	0.17
Maltose	9.60×10^5	2.86×10^6	3.23×10^6	2.78×10^6	3.06×10^6	5.28×10^6	0.08
Pyruvic acid	1.42×10^2	41.7	1.45×10^2	3.51	4.48×10^3	2.93×10^4	0.07
Succinic acid	1.38×10^6	1.19×10^6	1.98×10^6	4.70×10^4	2.73×10^6	2.05×10^6	0.02
Other metabolites							
Urea	2.74×10^7	2.52×10^7	2.76×10^7	2.07×10^7	2.52×10^7	2.42×10^7	0.10
Pyrophosphate	7.24×10^3	3.74×10^4	1.65×10^3	2.51×10^3	3.42×10^3	3.72×10^4	0.92

*Proceeded by the number 1, indicates the intensity value is less than 10,000 counts. The cutoff level for the signal intensity was 10,000; a lower value was considered as noise.

[1]LL indicates *longissimus lumborum* and PM indicates *psoas major*. LL0, PM0, LL3, PM3, LL7, and PM7 indicates the muscle type at their display d 0, 3, and, 7, respectively.

[2]*P*-value represents muscles × display time interaction.

be formed from purine metabolism. An increased concentration of uracil in PM than LL is suggestive of muscle-specific differences in rates of nucleic acid hydrolysis postmortem. In the current study, polar metabolites were extracted in methanol; however, some non-polar fatty acids were also detected. This can, in part, be attributed to the ability of methanol to extract some non-polar metabolites (Lisec et al., 2006). Fatty acids such as stearic acid, palmitoleic acid, and linoleic acid were lower in LL compared with PM. Further research is required to determine the role of fatty acids in postmortem muscle metabolism and meat color.

Conclusion

The gas chromatography-mass spectrometry based non-targeted metabolomic approach was utilized to understand the differences in color stability between LL and PM during simulated retail display. The results indicate that the GC-MS based metabolomic technique is a valuable tool to study the metabolite changes in muscles during storage. The differences in metabolite utilization between LL and PM can partially explain shorter color stability of PM. The metabolomics approach will improve our understanding of post-harvest processes such as effects of aging, temperature, and packaging on meat quality. Further, this method can be utilized to validate how the metabolites change with the addition of ingredients such as lactate or succinate in postmortem muscle. Future research using targeted-metabolomics will aid in quantification of metabolite levels in muscles. The application of other omics techniques such as proteomics and genomics, in combination with metabolomics, will help to characterize the role of biomolecules in postmortem meat biochemistry.

Literature Cited

AMSA. 2012. Meat color measurement guidelines. American Meat Science Association, Champaign, IL.

Belskie, K. M., C. B. Van Buiten, R. Ramanathan, and R. A. Mancini. 2015. Reverse electron transport effects on NADH formation and metmyoglobin reduction. Meat Sci. 105:89–92. doi:10.1016/j.meatsci.2015.02.012

Bertram, H., N. Oksbjerg, and J. Young. 2010. NMR-based metabolomics reveals relationship between pre-slaughter exercise stress, the plasma metabolite profile at time of slaughter, and water-holding capacity in pigs. Meat Sci. 84:108–113. doi:10.1016/j.meatsci.2009.08.031

Brown, M. V., J. E. McDunn, P. R. Gunst, E. M. Smith, M. V. Milburn, D. A. Troyer, and K. A. Lawton. 2012. Cancer detection and biopsy classification using concurrent histopathological and metabolomic analysis of core biopsies. Genome Med. 4:33. doi:10.1186/gm332

Cevallos-Cevallos, J. M., J. I. Reyes-De-Corcuera, E. Etxeberria, M. D. Danyluk, and G. E. Rodrick. 2009. Metabolomic analysis in food science: A review. Trends Food Sci. Technol. 20:557–566. doi:10.1016/j.tifs.2009.07.002

D´Alessandro, A., C. Marrocco, V. Zolla, M. D'Andrea, and L. Zolla. 2011. Meat quality of the longissimus lumborum muscle of Casertana and Large White pigs: Metabolomics and proteomics intertwined. J. Proteomics 75:610–627. doi:10.1016/j.jprot.2011.08.024

Faustman, C., and R. G. Cassens. 1990. The biochemical basis for discoloration in fresh meat: A review. J. Muscle Foods 1:217–243. doi:10.1111/j.1745-4573.1990.tb00366.x

Glancy, B., and R. S. Balaban. 2011. Protein composition and function of red and white skeletal muscle mitochondria. Am. J. Physiol. Cell Physiol. 300:C1280–C1290. doi:10.1152/ajpcell.00496.2010

Graham, S., T. Kennedy, O. Chevallier, A. Gordon, L. Farmer, C. Elliott, and B. Moss. 2010. The application of NMR to study changes in polar metabolite concentrations in beef longissimus dorsi stored for different periods post mortem. Metabolomics 6:395–404. doi:10.1007/s11306-010-0206-y

Joseph, P., S. P. Suman, G. Rentfrow, S. Li, and C. M. Beach. 2012. Proteomics of muscle-specific beef color stability. J. Agric. Food Chem. 60:3196–3203. doi:10.1021/jf204188v

Kaddurah-Daouk, R., and K. R. R. Krishnan. 2008. Metabolomics: A global biochemical approach to the study of central nervous system diseases. Neuropsychopharmacology 34:173–186. doi:10.1038/npp.2008.174

Kanani, H., P. K. Chrysanthopoulos, and M. I. Klapa. 2008. Standardizing GC–MS metabolomics. J. Chromatogr. B Analyt. Technol. Biomed. Life Sci. 871:191–201. doi:10.1016/j.jchromb.2008.04.049

Kim, Y. H., M. C. Hunt, R. A. Mancini, M. Seyfert, T. M. Loughin, D. H. Kropf, and J. S. Smith. 2006. Mechanism for lactate-color stabilization in injection-enhanced beef. J. Agric. Food Chem. 54:7856–7862. doi:10.1021/jf061225h

Koutsidis, G., J. Elmore, M. J. Oruna-Concha, M. M. Campo, J. D. Wood, and D. Mottram. 2008. Water-soluble precursors of beef flavour: I. Effect of diet and breed. Meat Sci. 79:124–130. doi:10.1016/j.meatsci.2007.08.008

Kushmerick, M. J., T. S. Moerland, and R. W. Wiseman. 1992. Mammalian skeletal muscle fibers distinguished by contents of phosphocreatine, ATP, and Pi. Proc. Natl. Acad. Sci. USA 89:7521–7525. doi:10.1073/pnas.89.16.7521

Ledward, D. A. 1985. Post-slaughter influences on the formation of metmyoglobin in beef muscles. Meat Sci. 15:149–171. doi:10.1016/0309-1740(85)90034-8

Lisec, J., N. Schauer, J. Kopka, L. Willmitzer, and A. R. Fernie. 2006. Gas chromatography mass spectrometry–based metabolite profiling in plants. Nat. Protoc. 1:387–396. doi:10.1038/nprot.2006.59

Madhavi, D. L., and C. L. Carpenter. 1993. Aging and processing affect color, metmyoglobin reductase and oxygen consumption of beef muscles. J. Food Sci. 58(5):939–942. doi:10.1111/j.1365-2621.1993.tb06083.x

McKenna, D., P. Mies, B. Baird, K. Pfeiffer, J. Ellebracht, and J. Savell. 2005. Biochemical and physical factors affecting discoloration characteristics of 19 bovine muscles. Meat Sci. 70:665–682. doi:10.1016/j.meatsci.2005.02.016

Mohan, A., M. C. Hunt, S. Muthukrishnan, T. J. Barstow, and T. A. Houser. 2010. Myoglobin redox form stabilization by compartmentalized lactate and malate dehydrogenases. J. Agric. Food Chem. 58:7021–7029. doi:10.1021/jf100714g

Nerimetla, R. S. Krishnan, S. Mazumder, S. Mohanty, G. G. Mafi, D. L. VanOverbeke, R. Ramanathan. 2017. Species-specificity in myoglobin oxygenation and reduction potential properties. Meat Muscle Biol. 1:1-12.

O'Keeffe, M., and D. E. Hood. 1982. Biochemical factors influencing metmyoglobin formation in beef from muscles of differing color stability. Meat Sci. 7:209–228. doi:10.1016/0309-1740(82)90087-0

Ramanathan, R., and R. A. Mancini. 2010. Effects of pyruvate on bovine heart mitochondria-mediated metmyoglobin reduction. Meat Sci. 86:738–741. doi:10.1016/j.meatsci.2010.06.014

Ramanathan, R., R. A. Mancini, and G. A. Dady. 2011. Effects of pyruvate, succinate, and lactate enhancement on beef longissimus raw color. Meat Sci. 88:424–428. doi:10.1016/j.meatsci.2011.01.021

Ramanathan, R., X. Guo, G. G. Mafi, U. DeSilva, and D. L. VanOverbeke. 2015. Quantification of beef longissimus and psoas muscle mitochondria using real– time polymerase chain reaction. Meat Sci. 101:161.

Rudell, D. R., J. P. Mattheis, and E. A. Curry. 2008. Prestorage ultraviolet-white light irradiation alters apple peel metabolome. J. Agric. Food Chem. 56:1138–1147. doi:10.1021/jf072540m

Sammel, L. M., M. C. Hunt, D. H. Kropf, K. A. Hachmeister, and D. E. Johnson. 2002. Comparison of assays for metmyoglobin reducing ability in beef inside and outside semimembranosus muscle. J. Food Sci. 67:978–984. doi:10.1111/j.1365-2621.2002.tb09439.x

Seyfert, M., R. A. Mancini, M. C. Hunt, J. Tang, and C. Faustman. 2007. Influence of carbon monoxide in package atmospheres containing oxygen on colour, reducing activity, and oxygen consumption of five bovine muscles. Meat Sci. 75:432–442. doi:10.1016/j.meatsci.2006.08.007

Subbaraj, A. K., Y. H. B. Kim, K. Fraser, and M. M. Farouk. 2016. A hydrophilic interaction liquid chromatography–mass spectrometry (HILIC–MS) based metabolomics study on colour stability of ovine meat. Meat Sci. 117:163–172. doi:10.1016/j.meatsci.2016.02.028

Tang, J., C. Faustman, T. A. Hoagland, R. A. Mancini, M. Seyfert, and M. C. Hunt. 2005. Postmortem oxygen consumption by mitochondria and its effects on myoglobin form and stability. J. Agric. Food Chem. 53:1223–1230. doi:10.1021/jf048646o

Warner, R. D., R. H. Jacob, K. Rosenvold, S. Rochfort, C. Trenerry, T. Plozza, and M. B. McDonagh. 2015. Altered post-mortem metabolism identified in very fast chilled lamb M. longissimus thoracis et lumborum using metabolomic analysis. Meat Sci. 108:155–164. doi:10.1016/j.meatsci.2015.06.006

Wishart, D. S. 2008. Applications of metabolomics in drug discovery and development. Drugs R D. 9:307–322. doi:10.2165/00126839-200809050-00002